International Academy of Science,
Engineering and Technology
Connecting Researchers; Nurturing Innovations
IASET

AN EXPERIMENTAL STUDY OF TURBULENT SEPARATION FLOW AND HEAT TRANSFER IN A CIRCULAR CONCENTRIC ANNULUS

Yasin K. Salman & Hussam Fiesal Abed Hmood

Research Scholar, Department of Mechanical Engineering, College of Engineering, University of Baghdad, Baghdad, Iraq

ABSTRACT

The step height effect of radially inward expanded air flow stream on the heat transfer process in a concentric circular annular passage is studied experimentally. The air flow separation, reattachment and redevelopment took place in the test section which its inner tube subjected to a constant heat flux boundary condition. The experimental apparatus comprised of concentric tubes to form an annular passage with a sudden enlargement in the passage cross-section created by increasing the outer tube diameter of the annular inner tube at the entrance section prior to the test section. The inner tube of the test section was made of aluminium having 25 mm outside diameter and 350 mm heated lengths, which was subjected to a constant wall heat flux boundary condition.The investigation was performed to cover a Re range of 3000 – 11000, inner tube heat flux varied from 800 W/m^2 to 1750 W/m^2 and the enhancement of step heights were S = 0 (without step), 6.5 mm, 12.5 mm, and 18.5 mm which refer to D_i/d = 1, 1.5, 2 and 2.5, respectively.

Results reveal for all cases, that the local heat transfer coefficient increased against increasing the heat flux and/or Re. The step height has an eminent effect on heat transfer in the separation region which decreases with the raise of the step height. The passage without step (S=0) results were correlated and compared with the availableturbulentforced convectionentry length correlations for same geometry and boundary conditions. The step height effects show, for S= 6.5 mm a 25% on the average improvement in heat transfer for a full Reynolds number tested while for another two step heights the results show a limited improvement in low Reynolds number to a 16.5% reduction in heat transfer due to separation zone effect. The velocity profiles demonstrate that the position of reattached point behind the step increases with the rise of step height.The present results show a good agreement with the available previous works and have followed similar trends.

KEYWORDS: *Turbulent Forced Convection, Internal Flow Separation, Concentric Annular Passage*

INTRODUCTION

The separation of boundary layer takes place when the part of the boundary layer close to the wall reverse in flow direction and that occurs as the overall boundary layer thickens suddenly to force it off the wall by the reverse flow. For internal flow, such as a rapid expansion of pipe, an adverse pressure gradient met as the flow expands creating an extended region of separated flow. Separation generates two parts; the recirculating flow and dividing streamline at the central region of the pipe. The point at which the dividing streamline attached the wall is called the reattachment point. As the flow goes further downstream, it eventually redevelops and settles down to achieve an equilibrium state [1]. The flow separation as one of the viscous flow problems is very important for science and industry. As per classical concept, flow separation is

caused due to viscosity. Therefore, it is often expressed as "boundary layer separation". Generally there are two types of flow separation, separation of external and internal flow [2]. The classification of separation can also sort related to flow behaviour as separation with or without reattachment. Typical examples of the former are the flow over a backward facing step, the leading – edge separation bubbles of air foils and blunt plates or blunt circular cylinders. The separation flow described as reattaching when the interaction exists between the vortices and the solid surface and it described as without reattaching when the interaction is between vortices shed from the separation point [3]. In general, this phenomenon is encountered in some engineering applications, such as flow over air foils at large angles of attack, in channels where area suddenly increases, in wide angle diffusers [4–9], heat exchangers, combustors, nuclear reactor cooling channels [10], in power plants [11], gas turbines and electronic circuit panels [12–13].

Forced convection heat transfer in a concentric circular annular passage has been studied experimentally and analytically by Kays and Leung [14]. The experimental solutions established for air flow with thermally entry length and second kind boundary conditions and employed in a broad range of Reynolds numbers with either outer tube heated or inner tube heated with constant heat flux. The experimental data converted to an empirical equation which was in a good agreement with analytical solutions. A correlation equation has been presented for air flow in annular passage with constant heat flux subjected to the inner tube only and for annulus radius ratio r* = 0.2 (r*=r_i/r_o) for as asymptotic Nusselt number as:

$$Nu_{Dh} = 0.0324 \, Re_{Dh}^{0.762.} \dots\dots\dots\dots\dots\dots\dots\dots\dots\dots\dots\dots \quad (1)$$

Using THMOD2 code, Bsebsu and Bede [15] presented a theoretical investigation dealing with a down flow single-phase forced convection in a narrow vertical annuli sub channel (WWR-M2 channel). The investigation main objective was to examine the applicability of available turbulent heat transfer equations in a narrow vertical annuli channel. The module represents a 3 mm spacing (gap) and 600 mm active length in fuel elements used in thermal hydraulic analysis tasks of the WWR-M2 research reactor. The investigation concluded that by using the equivalent hydraulic diameter the existing correlations are applicable to WWR-M2 channel. A new equation has also been developed for sub channels of WWR-M2 for either one or both side heated conditions.

The heat transfer characteristic in a double pipe with 560 pin fin heat exchanger was studied theoretically by Nieckele and Saboya[16]in which the air is flowing in the annular channel while the water is flowing in the inner circular pipe. The results depicted in dimensionless form and in terms of average Nusselt number and friction factors as a function of the Reynolds number ranging from 13,000 to 80,000. A comparison with the available smooth sections was presented. Filetti and Kays [17] experimentally studied the local heat transfer rates to air flow close to the entrance of a flat duct in which there is an abrupt symmetrical enlargement at the flow cross section. Reynolds numbers varied from 70,000 to 205,000 and two enlargement area ratios (2.125 and 3.1) were considered.It was found that such a flow was characterized by a long stall on one side and a short stall on the other. Maximum heat transfer occurs in both cases at the reattachment, followed by decay towards the values for fully developed flow. The results also revealed that the Nusselt number along the annulus inner tube downstream the step for the separation, reattachment and redevelopment regions has the same behavior as described by Vogel and Eaton [12]. Heat transfer in the separation region behind an obstacle was studied experimentally by Davletshin et al. [18]fora wide frequency range of superimposed free stream pulsation. The heat transfer coefficient was evaluated by solving an inverse non-stationary heat conduction problem based on experimentally measured, the wall transient temperature. The pulsation flow shows substantial heat transfer intensification in the separation region.

The effect of Reynolds number and the duct divergence angle on the flow separation characteristic in a conical duct was studied numerically by Sparraw et al [19]. The flow considered as fully developed at the diffuser inlet while the diffuser exit connected to a long circular pipe. A moderate-turbulence and transition Reynolds number at the diffuser inlet accommodated to get a possible laminarization of flows using a universal flow regime model. The investigation outcome found that the separation angle for Reynolds number less than 2000 occurs with a diffuser expansion angle of 5 degrees. The results conceal a prior guideline that separation first occurs at a divergence angle of 7 degrees. The simulation shows that for divergence angle from 20 to 30 degrees, the separation occurs in all investigated Reynolds numbers. Togun et al. [20] investigated experimentally the effect of step height on the outward separation air flow in a concentric annulus in which the annulus outer surface is subjected to a constant heat flux. Investigation covered in a Re range of 17050-44545, heat flux varied from 719 W/m^2 to 2098 W/m^2 and the enhancement of step heights were, S= 0 (without step), 6 mm, 14.5 mm and 18.5 mm, which refer to d/D = 1, 1.16,1.53 and 1.80, respectively. The effect step height of flow separation has been correlated and the results reveal that the maximum enhancement of 18% occurs for step height 18.5 mm. Local heat transfer coefficient demonstrates a gradually improving in heat transfer directly after the step in the separation region to reach maximum value in the reattached point then it decreases gradually as the boundary layer builds-up in the redeveloped region.

The entry lengths for turbulent flow are typically short in comparison with the laminar flow entry length often just 10 tube diameters long, and therefore the Nusselt number determined for fully developed turbulent flow can be used approximately for the entire tube. This simple approach gives reasonable results for heat transfer for long tubes and conservative results for short ones. The correlation for the average heat transfer coefficient in a short annulus is very limited and the condition of applying notorious equation of Dittus and Boelter [21] is far from the present experiment condition. Therefore, to compare the present experimental result, the empirical equation should be taking into account the effect of Reynolds and Prandtl numbers, the position of the passage entrance, and the annulus side heated. Petukhov [22] and Gnieliski [23] correlate for circular tube and the available data somewhat better than any other over the range of Prandtl number from 0.5 to 2000, and Reynolds number from 2300 to 5x10^6. Kim et al. [24] recommended the following empirical equation for the low turbulent Reynolds number forced convection heat transfer in the entrance of the annulus:

$$\mathbf{Nu = 0.039 \, C_{Therm} Re_D^{0.74} \, Pr^{0.4}} \dots\dots\dots\dots\dots\dots\dots\dots\dots\dots\dots\dots \tag{2}$$

WhereC_{Therm} is a function of Re and the normalized distance from the start of the heating zone, x/D$_h$, where D$_h$ represents the hydraulic diameter:

$$\mathbf{C_{Therm} = 1.0 + exp\left(0.08 * \left(\frac{x}{D_h}\right)\right)\left(\frac{x}{D_h}\right)^{-0.25}\left[0.65 + \left(\frac{2925}{Re}\right)\left(\frac{x}{D_h}\right)^{-0.3}\right]} \dots\dots\dots\dots \tag{3}$$

Low Reynolds turbulence model results are compared with the experimental data available and the predicted by v²-f model and the comparison was found much closed. A correction to the above forced convection equation is suggested by Petukhov and Roisen [25] for the annulus with inner tube wall heated with constant heat flux while the outer wall is insulated:

$$\mathbf{\frac{Nu_c}{Nu_F} = 0.86 \left(\frac{D_o}{D_i}\right)^{0.16}} \dots\dots\dots\dots\dots\dots\dots\dots\dots\dots\dots\dots\dots \tag{4}$$

Where Nu$_F$represents the output of the equation presented by Petukhov [22] or Gnieliski [23]for circular tube while Nu$_c$ is the correctedNusselt number value for an annulus has the outside diameter D$_o$ and the inside diameter D$_i$.

There is a shortfall of experimental observation to describe the separation and heat transfer processes in annular passage especially for short passage. The motivation of present investigation is to add a modest contribution to the flow separation phenomenon. This work focuses to study the effect of flow separation of the heat transfer process for an axisymmetric, transient to turbulent separated flow in an annular passage. The air flow separation was induced with different heights of circular steps by increasing the inner annular tube diameter at upstream of the heated test section. Reattachment and redevelopment of the flow occurred behind the point of separation. The test pipe was heated electrically to conduct the experiments at constant heat flux and the degree of separation is varied by using different tube diameters while the Reynolds number was maintained in the same range by regulating the gate at the entry of the blower.

Experimental Apparatus

The apparatus was designed and constructed to have an axisymmetric separated and reattached air flow in an annular passage. The full set-up with annular shaped test section is shown in Figure 1. The passage proceeds upstream with a variable entrance calming section. The apparatus can provide different air velocities (variable Reynolds numbers) and heat fluxes at the test section. In general, the apparatus consists of two parts, the open air circuit and the measuring system (Table 1).

An open-air circuit, as shown in Figure 2, consists of a small centrifugal fan (A), delivery section (B), settling chamber (C) and the circular concentric annular tubular passage (D, E and F). The annular passage has started with an entrance section (D) and has ended with an exit section (F). The air delivered by a variable speed centrifugal fan (A) and was controlled by a fan speed regulator (Variac) and fine adjusting the position of the lever of the inlet gate valve (G) at the fan entrance. The velocity of the air was measured by using a hot wire anemometer (H) located at the end of thecircular delivery section (B). Air then passes through the settling and the calming section (C) which equips with two layers of fine gauze (I) and a layer of the flow straightener (J) to streamline the incoming air before delivering it to the passage bell mouth (K). Then, the air passes through the circular concentric tube annular passage (D to F). It is constructed of an unheated aluminum outer tube (Q) of constant inner diameter of (140 mm) and elongated to cover all the annular passage while the passage inner part has two tubes with variable diameter tube (M) located at annulus calming entrance section and the heated test tube (L) with constant diameter of (25 mm) located at annulus passage test section. Both tubes held and supported horizontally and centrally with the help of the threaded rod (N) which rested in the exit centered Teflon piece (R2) and fasten withhexagonal nut (O2) from one side while the other side rested on the cross metal piece (P) in the settling section and fasten with hexagonal nut (O1). This combination allows the passage inner tube to be assembled and dismantled easily for changing the entrance section inner tube and to adjust its position horizontally and centrally in the passage. The calming entrance section inner tube outer diameter varies according to the separation step height case study. It has four variable diameters D_i of 25, 37.5, 50 and 62.5 mm which provides a separation diameter ratio (D_i/d) of 1.0 (with no separation), 1.5, 2.0 and 2.5, respectively. The combination of annulus inner tube (M) and the two Teflon pieces (R1) (connecting the two tubes (M) and (L) and on which separation takes place) and (R3) (adopted with the bell-mouth (K) to minimize the flow disturbance at the annular passage entrance) is sliding on the threaded rod during the assembly. The annulus outer tube (Q) in the test section part has seven holes (W) which allow the Pitot static tube to be penetrated during the velocity profile test. The Pitot Static tube is connected with the micro-manometer via a flexible connection (U). To measure the bulk air temperature at the passage inlet and outlet, four thermocouples have been inserted in the flow passage one thermocouple (S1) to measure the air inlet temperature and three thermocouples (S2) to measure the bulk air temperature at the passage exit.

The air at the test section E, (which is the last part of the open air circuit) experienced a separation, reattachment and redevelopment at the passage downstream. It was heated by the annulus inner tube of that test section (L) at constant heat flux (CHF). The outer surface of connecting Teflon pieces (R2) was especially machined to be flush mounted with both calming section inner tubes (M) and test section inner tube (L) to prevent any flow disturbance at the separation point. Teflon was chosen for easy machinability and low thermal conductivity in order to reduce the test section end losses. All pieces were machined from a Teflon rod (75 mm) in diameter. Two layers of fibre glass (40 mm thickness) were used to cover the outside surface of the annular passage outer tube (Q) to reduce the heat losses radially outwards the annular passage. The fan discharges the air to the system via a flexible connection (V) to prevent fan vibration to be transmitted to the system.

Heating System

The test tube was heated electrically by using an electrical heater as shown in Figure 3. The heater consists of a nickel–chrome (Nickhrom) wire (A) uniformly wounded to produce a constant heat rate per unit length. The heater was isolated electrically from the aluminium tube (B) by winding with a very thin asbestos tape and the wire itself was isolated by fine ceramic beads. A 10 mm wide tape spacer has been wounded while winding the heater to assure uniform heater winding. The temperature along the outer tube surface was measured by 16 thermocouples (D) located along the tube, starting from the separation point $(X = 0)$ up to the end of the test section as shown in Figure 3. At first, thermocouple positions were marked along the entire tube surface, and then 1.5 mm holes were drilled on the wall at 2 mm depth. The drilled holes were then chamfered by a 2 mm drill and cleaned properly. Thermocouples hot junctions (E) were inserted inside the tube and installed and secured in cleaned holes with adhesive (F). The outer surface of the test tube then cleaned to remove the excess adhesive and to make the measuring point flash mounted with the tube surface.To avoid convection currents in the space between the heater and the cylinder inner surface, this space is filled and compacted with magnesium oxides (C). Magnesium oxide was selected as it has relatively high thermal and poor electrical conductance.

To determine the heat loss by conduction from the test tube ends to the Teflon pieces, two thermocouples (G1 and G2) inserted on each side of the test tube in the end Teflon pieces (H1 and H2) as shown in Figure 3. Knowing the thermal conductivity of Teflon and the distance between the thermocouples, the end conduction could be calculated. The maximum value of this, varied in the experiments between 1.23% and 2.5% of the total heat input. To evaluate the conduction heat loss from the whole fiber glass insulation cover the whole passage, the average temperature of the four thermocouples (I) under fiberglass of the test section and the average temperature of two other thermocouples located (2 mm) apart from the first two were recorded. Then, by knowing the fiber glass thermal conductivity, the heat losses could be calculated. The amount of heat loss varied in the experiments and the maximum value of this was less than 0.25% of the total heat input. All thermocouples used in the test rig are K type, 0.1 mm diameter wire and with two-layers of asbestos insulation.All the thermocouples were calibrated in the laboratory using the boiling and melting point of pure chemical substances. The thermocouples were calibrated without lead and with lead (similar to experiment condition) to determine the correction factor for applying leads and the results show no appreciated effect on the calibration. The thermocouples were made by fusing the ends of two wires by an electric spark in an oxygen free environment.

Data Analysis Method

The following simplified steps were used to evaluate the heat transfer to the flowing air in the expanded annular passage while the inner surface of outer tube was subjected to uniform wall heat flux boundary conditions. The total heat

transfer can be calculated using:

$$Q_T = V.I \dots\dots\dots\dots\dots\dots \tag{5}$$

The convection and radiation heat transferred from the test section inner tube surface is calculated by:

$$Q_{c+r} = Q_T - Q_{cond} \dots\dots\dots\dots\dots\dots \tag{6}$$

Where Q_{cond} is the conduction heat losses through Teflon end pieces and Q_{c+r} is the convection and radiation heat transfer. The conduction heat transfer from fibre glass can be represented by:

$$Q_{cond} = k_{Teflon}A_{Teflon}\frac{\Delta T_{Teflon}}{\Delta x_{Teflon}}\dots\dots\dots\dots\dots\dots \tag{7}$$

Where ΔT_{Teflon} is the temperature difference inside each of the test tube Teflon end pieces, Δx_{Teflon} represents the distance separate the thermocouples, k_{Teflon} is the Teflon thermal conductivity and A_{Teflon} represents the Teflon end piece cross-sectional area.

The convection and radiation heat flux can be represented by:

$$q_{c+r} = \frac{Q_{c+r}}{A_s} \quad \dots\dots\dots\dots\dots\dots \tag{8}$$

Where $A_s = \pi d L$, L and d represent the test tube length and diameter, respectively. The radiation heat flux can be represented by the following Eq.:

$$q_r = \sigma F_{12}\left(T_{a1}^4 - T_{a2}^4\right)\dots\dots\dots\dots\dots\dots\dots \tag{9}$$

Where σ is the Stefan–Boltzmann constant (5.669×10^{-8}W/K^4 m^2); while F is the shape factor is equivalent to:

$$F_{12} = \frac{1}{\left(\frac{1}{\varepsilon_1}\right)-\left(\frac{A_1}{A_2}\right)\left(\frac{1}{\varepsilon_2}-1\right)}\dots\dots\dots\dots\dots\dots \tag{10}$$

ε_1 and ε_2 are the annulus surface emissivity values (outer surface of the annulus inner tube and the inner surface of the annulus outer tube in the test section), T_1 is the average outer surface of the test section inner tube temperature and T_2 is the average inner surface of the test section outer tube temperature. The convection heat flux can be represented by:

$$q_c = q_{c+r} - q_r \dots\dots\dots\dots\dots\dots \tag{11}$$

The convection heat flux is used to calculate the local and average heat transfer coefficients as follows:

$$h_X = \frac{q_c}{(T_{SX} - T_{BX})} \dots\dots\dots\dots\dots\dots \tag{12}$$

All the properties were evaluated at the mean film temperature which evaluated by the following Eq.:

$$T_{fX} = \frac{T_{SX} - T_{BX}}{2}\dots\dots\dots\dots\dots \tag{13}$$

Where T_{BX} is the local bulk air temperature and T_{fX} is the local mean film temperature.

The local Nusselt number based on the diameter ($Nu_{X,Dh}$) can be determined by:

$$Nu_{X,Dh} = \frac{h_X Dh}{K_f} \dots\dots\dots \tag{14}$$

The local Nusselt number based on the axial distance (Nu_X) can be evaluated by the following Eq.:

$$Nu_X = \frac{h_X X}{K_f} \ldots\ldots\ldots\ldots \qquad\qquad \ldots\ldots\ldots\ldots\ldots\ldots..(15)$$

The average values of the Nusselt number (Nu_L) can be calculated based on the calculated average heat transfer coefficient by:

$$h_L = \frac{1}{L}\int_0^L h_X.\,dx \ldots\ldots\ldots\ldots \qquad\qquad \ldots\ldots\ldots\ldots\ldots\ldots (16)$$

The average Nusselt number based on the calculated average surface temperature and average bulk air temperature are evaluated:

$$h_L = \frac{q_c}{(T_{SL} - T_{BL})} \ldots\ldots\ldots\ldots \qquad\qquad \ldots\ldots\ldots\ldots\ldots\ldots. (17)$$

Where

$$T_L = \frac{1}{L}\int_0^L T_X.\,dX \ldots\ldots\ldots\ldots \qquad\qquad \ldots\ldots\ldots\ldots\ldots\ldots.. (18)$$

$$T_{BL} = \frac{T_{X=L} + T_{X=0}}{2} \ldots\ldots\ldots \qquad\qquad \ldots\ldots\ldots\ldots\ldots \ldots\ldots. (19)$$

All the average properties were evaluated at the mean film temperature as:

$$T_{fL} = \frac{(T_L - T_{BL})}{2} \ldots\ldots\ldots\ldots\ldots\ldots\ldots\ldots\ldots\ldots \qquad\qquad \ldots\ldots\ldots. (20)$$

The local Reynolds number based on the hydraulic diameter (Re_{Dh}) can be calculated by:

$$Re_{Dh} = \frac{\rho_f.U.Dh}{\mu_f} \ldots\ldots\ldots\ldots\ldots \qquad\qquad \ldots\ldots\ldots\ldots\ldots\ldots.. (21)$$

And the local Reynolds number based on the distance (Re_x) can be determined by:

$$Re_x = \frac{\rho_f.U.X}{\mu_f} \ldots\ldots\ldots\ldots\ldots\ldots \qquad\qquad \ldots\ldots\ldots\ldots\ldots. (22)$$

All the air physical properties ρ_f, μ_f, v_f and k were evaluated at the average mean film temperature ($\overline{T}_f$) Holman (2010) [8]. A computer program in FORTRAN was written with algorithm capable to manipulate the data set calculation of air all properties locally and doing and select best equations which fit surface temperatures and local heat transfer coefficients and then doing the numerical integration to obtain the average value for heat transfer coefficient and dimensionless groups for the whole cylinder.

RESULTS AND DISCUSSIONS

To cover all experimental parameters, check the measurement consistency and to test the velocity profile variation along the passage, a total of 70 test runs were conducted. The parameters to cover include a straight annular passage without step (S = 0) and three passages with step heights corresponding to S = 6.5mm, 12.5 mm and 18.5 mm hold the passage expansion ratios $(D^2\text{-}d^2) / (D^2\text{-}D_i^2) = 1$, 1.045,1.11 and 1.2 respectively. The test section inner tube heat flux was varied from 800W/m^2 to 1750 W/m^2 while Reynolds numbers Re_Dwasvaried from 3000 to 11000. The velocity profile test runs cover the annular passage with steps and for seven axial positions. The data reproducibility is good and remains within the confidence level of 95% and average rms error less than 1.5%.

Variation of Surface Temperature

The variation of surface temperature along the test section inner tube which may affected by many variables, such as flow velocity, surface heat flux and upstream flow separation created by the step. The temperature variations for a selected runs are demonstrated in Figure 4,5 and 6.

Figure 4 shows the surface temperature variations along the test section heated inner tube for different heat fluxes with a specific Re_D = 3000 and step height S=18.5 mm i.e. (D_i/d = 2.5). The general distribution shows a reduction of surface temperature immediately behind the step at the test section entrance (x = 0) to reach the minimum value at specific axial position at which the flow reattachment expected to occur after the separation region due to the turbulence which increased the heat transfer. The surface temperature then increased gradually to reach a maximum value then it decreases at the test section exit due to the tube end losses.

Figure 5 depicts the variation of Re number effect on the temperature distribution of the test section inner tube at specific heat flux equal to 1750W/m^2 and step height equal to 18.5 mm. The figure reveals that the surface temperature decreases as the Re_D increases for the same heat flux and step height.

Figure 6 presents the temperature distributions for selected runs using the step height as a variable parameter. It is detected that while the surface temperature for the straight passage increased gradually for whole the heated surface the other three cases show that the surface temperature increases as the step height increases especially in the separation region, directly behind the step for the same Reynolds number and surface heat flux. The figure also reveals that the position of the minimum surface temperature moves downstream as the step height increases to indicate that the separation region behind the step increases as the step height increases. The surface temperature distribution over the separation region has a similar trend of a straight annulus case with a gradual increase of surface temperature for the rest of the tube. The minimum temperature represents the expected flow reattached point. Separation produces a recalculated flow moving towards the step at the heated tube surface which then drifts away from the step by the main separated flow.

Evaluation of Local Heat Transfer Coefficient (h_X)

The variation of the local heat transfer coefficient h_X along the test section inner tube (X) for selected runs is shown in Figure 7 and 8. Figure 7 depicts the effects of Reynolds number variation on the h_X distribution for a corresponding heat flux equal to 1750 W/m^2. Thedistribution of local heat transfer coefficient $h_X$increases until it reaches a maximum value at the reattachment point (maximum local heat transfer point) after which h_x decreases to grow asymptotically while moving downstream along the X-axis towards the test section exit.

Figure 8 shows the variation of local heat transfer coefficient h_X with straight annulus (without step) and three different expanded passages due to different step heights. The straight annulus shows completely different distribution compared with the other cases (with step) as the distribution decreases sharply at the test section entrance then decreases gradually to end asymptotically at the section exit. The high h_X at x=0 is due to zero thermal boundary layer at the test section entrance. For separated flow (with step) and same Reynolds number and heat flux, the local heat transfer coefficient $h_x$increases as the step height increases, especially in the separation region due to still recirculating induced vortex which move towards the step at the inner tube surface and drifting away by the separated flow. The still recirculating vortex reduces the heat transfer rate directly behind the step. The figure also reveals that $h_X$values for D_i /d equal to 1.5 shows a quite improvement in heat transfer rate in comparison with straight annular passage and that attributed

to a limited and unclear separation zone for this step height and this step height also increases the case turbulent intensity. The other two cases (D_i /d equal 2.0and 2.5) show different behaviour as in the separation region, the decline of h_X is quite clear in comparison to h_X obtained for the flow in a straight annular passage.

Flow Profiles

The variation of velocity profiles for the separated flow along the test section annular passage and for three step heights 6.5 mm, 12.5 mm and 18.5 mm are presented in Figs. 9, 10 and 11, respectively. The three figures are presented for the same Reynolds number equal to 5000 and same heat flux equal to 1750 W/m^2.Each figure comprises a seven profiles at X equal to 0 mm (at the test section entrance), 25 mm, 50 mm, 75 mm, 125 mm, 175 mm and 225 mm. The profile shows the variation of dimensionless axial velocity U* against the dimensionless radial position R* when r measured from the annulus center line.

Figure 9 reveals that all the profiles in this figure have covered the entire passage with the profile at the test section entrance (X/D_h = 0) shows that the flow could be regarded as a fully developed turbulent annulus flow for Re > 2000. The lower part of the profile at X/D_h equal 0.215 just behind the step is sharply retreat and the first radial position near the tube surface is hardly to measure as the micro-manometer recorder shows unsettled reading with a lot of fluctuation due to higher expected turbulence intensity. Due to expected symmetry, the other profiles show a clear progressive development in the internal part annular boundary layer adjacent to the test section inner tube. The flow behaviour combined with the result of the temperature distribution reveals a very limited separation zone for this step height.

For step height D_i /d, Figure 10 also shows the profile at the test section entrance (X/D_h = 0) could be regarded as a fully developed turbulent annulus flow. The lower part of the first profile at X/Dh equal 0.215 just behind the step is also sharply retreat and the first radial position near the inner tube surface is fluctuating around zero and hardly to measure which indicates that the flow in this goes in the opposite direction and it is not a part of the main flow.The spatial growth of velocity fluctuations from the measurements demonstrated a tendency that casting a vortex behind the step. Therefore, this profile is left uncompleted as the lower part of it is dominated by recirculating vortex in the flow separation zone. The other profiles show clear progressive development of the boundary layer adjacent to test section inner tube. The reattachment length could be extended between axial local position X equal to 25mm and 50 mm.

Figure 11 shows the velocity profiles variation along the test section for step height of 18.5 mm (D_i /d = 2.5) which reveals that the profile at the test section entrance (X/D_h = 0) could be regarded as a fully developed turbulent annulus flow and the reattachment length increases as the step height increases as the second and third profiles suffer a sharp retreat while first two local radial positions in the second profile and first local position in the third profile near the inner tube surface is fluctuating around zero and showing a reverse flow to the main passage flow. Again the other profiles show a progressive development of the annular inner boundary layer. The reattachment length behind the step could be extended between the axial local position X equal to 50mm and 75 mm.

Development of Average Heat Transfer Correlation

To estimate the effect of step height on the present experimental data, it is required first to correlate the straight circular annular passage data (without step) and compares it with the available equations dealing with the present geometry and boundary conditions.The correlation for the average heat transfer coefficient in a short annulus and annulus entry

length is very limited and the conditions of applying Dittus and Boelter [21] equation (fully developed flow) are far from the present experimental condition. All the references indicated that the result of heat transfer at the entrance region (developing flow) is higher than the fully developed flow for both laminar and turbulent flows. The result obtained by applying Petukhov [22] and Gnieliski [23] (for Re>2500) correlations and the correction for annular passage Eq. (4) suggestedby Petukhov and Roisen [25] is approximately equal to the Eq. (2) recommended byKim et al. [24]. Figure 12 shows the present correlation for the present straight annulus with inner tube subjected to constant heat flux is compared with both Kim et al. [24] Eq.(2) and the well-known fully developed flow proposed by Dittus and Boelter [21] equation. The figure shows that the results of the present correlation are higher than the results obtained by applying Eq. (2) in the range from 5% to 14% for the whole applied Reynolds number.

The relationships between the average Nusselt number ($Nu_{L,Dh}$) and the average Reynolds number ($Re_{L,Dh}$) are shown in Figs. 12–13 to represent the measured heat transfer along the whole test section tube (separation, reattachment and redevelopment regions) for different step heights. The whole range of Reynolds numbers and heat fluxes are covered. The coefficients of these correlations are presented in Table 2, and the general correlation equation is presented in Eq. (23).

$$\mathbf{Nu_{L,Dh} = C\,Re_{L,Dh}^{n}} \dots\dots\dots\dots \qquad\qquad \dots\dots\dots\dots\dots\text{(23)}$$

For step height 6.5mm (Di $_{/}$d = 1.5), the correlation shows an improvement in heat transfer process for full experimental range of Reynolds and it varied from 41.5% to 9.7% as Reynolds number changed from 3000 to 11000. The correlations for another two step heights show a limited improvement in heat transfer at low Reynolds which at Reynolds number equal to 3000 equivalent to 12.4% and 4.08% at step height 12.5 mm and 18.5 mm, respectively. For the Reynolds number 11000 both steps show a reduction in heat transfer which equivalent to -16.84% and -16.34%at step height 12.5 mm and 18.5 mm, respectively.

Figure 14 shows a correlation between the local maximum Nusslt numbers based on D_h divided by dimensionless parameter (D_h/S) with the local Reynolds number based on D_h. The correlation shows the relation between the maximum local heat transfer coefficient $h_{X,max}$, step height S and the Reynolds number based on D_h. The linear fit of the experimental data for the three steps is presented by the following equation:

$$\boldsymbol{Nu_{max,Dh} = 0.0346\,Re_{Dh}^{0.619}\left(\frac{Dh}{S}\right)} \dots\dots\dots\dots\dots\dots \qquad \dots\text{(24)}$$

CONCLUSIONS

From the experimental investigation into the range of Reynolds numbers, heat fluxes and step heights, the following conclusions can be drawn:

- In comparison with the straight passage (without step), the surface temperature distribution for step annular flow shows a notable increase in magnitude for same Re number and heat flux and the increase rises with the increase of step height.

- Increase the step height and the flow causes the surface temperature coming down up to a specific point (lowest temperature) along the test section inner tube and it then increases. The lowest temperature represents the flow reattachment point. The position of the lowest temperature is mainly a function of step height.

- The local heat transfer coefficient (h_X) increases as the Reynolds number increases for all cases with or without

step. In the separation region (recirculation zone) the local heat transfer coefficient improves until it reaches a maximum value ($h_{X,max}$) at the flow reattachment point.

- Reynolds number variation has limited effect on the flow reattach point in comparison with the step height and an increase of the flow Reynolds number moves the reattachment point downstream away from the step. The location of maximum heat transfer coefficient moves downstream as the step height increases.

- Flow velocity profiles reveal that the low step heighttested (S = 6.5 mm) does not demonstrate a clear separation zone with a clear recirculation flow behind the step in comparison with the other high step height cases (S = 12.5 mm and S = 18.5 mm)

- Average Nu number and Re number can be correlated for all cases (with or without step) of flow configuration in the annular space. The maximum Nu number, step height and Re number can also be correlated for all with step cases.

ACKNOWLEDGMENTS

Table 1: Specification of Equipment and Measuring Instruments

Instrument	Specifications
Micro-manometer	Furness Controls ltd, Type FCO14, Model 1, total resolution 10 1:20,000, accuracy ±.0004"H2O, 12" Pitot static probe and connections.
Hot-wire anemometer	E+E elecktronic,EE75, Model B,0-40 m/s, ±0.03 m/s
Analog Ammeter:	Goerz, Type 324760, No. 691907
Centrifugal Fan	Marquis Type, : 3Ø phase, 6/7 (m3/min), power 0.3 kW
Digital Voltmeter	Philips, Type PM2404, ±0.83% full scale
Digital Electronic Thermometer	Comark, Type No. 6110, serial No. 11725, Resolution 0.1 C
Heater	Nickel Chrome wire (NIC80-040-250) 1 mm Dia.
Transformer (Variac)	Lubcke, Type R52, No. 531.51
Selector Switch	Comark Type No. 1695, serial No. 24054& Comark Type No. 1695, serial No. 11725
Thermocouples wires:	Two layers Glass covered Iron-constantan Type k 0.3 mm Dia.

Table 2: Values of S, C and Slop n at Different Step Height

Diameter Ratio (D_i/d)	Step Height S mm	C Value	Slop n
1	0	0.197	0.664
1.5	6.5	1.339	0.468
2	12.5	1.419	0.432
2.5	18.5	0.787	0.496
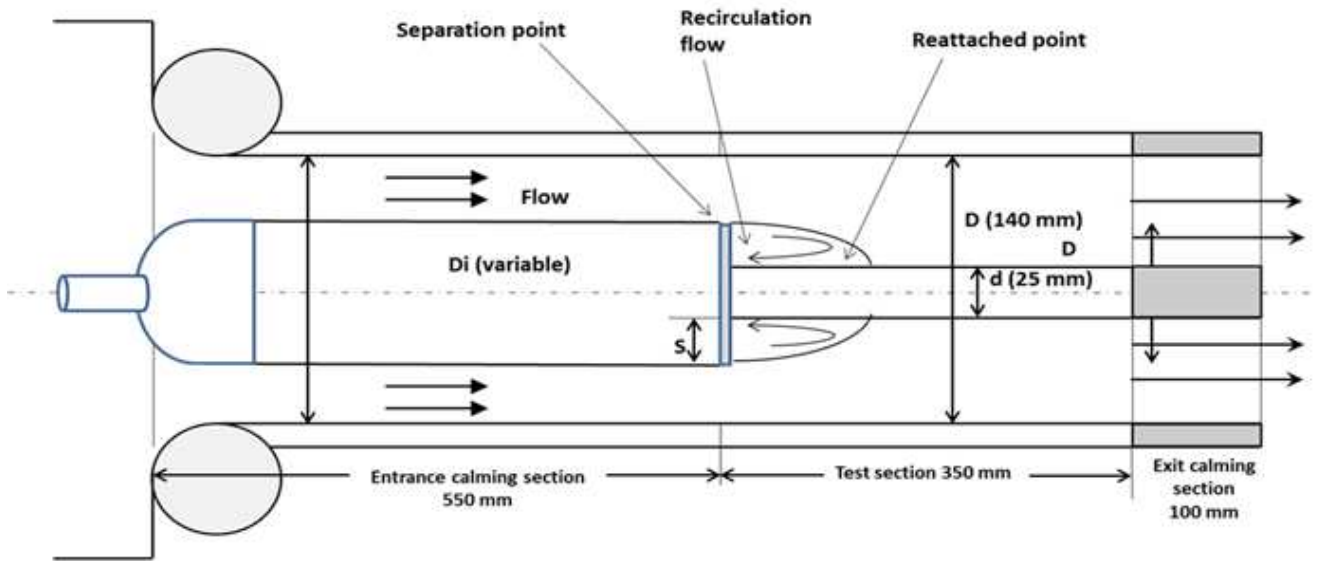
Figure 1: Annular Passage Configuration and Dimensions

SYMBOL	DEFINITION
O1 & O2	Hexagonal Bolts
P	Cross Piece
Q	Whole Annular Passage Outer Tube
R1,R2 & R3	Teflon Pieces
S1 & S2	Bulk air inlet and outlet measuring
T	Pitot static Tube
U	PVC tube To micro-manometer
V	flexible connection
W	Outer tube holes for Pitot pentration

SYMBOL	DEFINITION
A	Centrifugal Fan
B	Delivery Section
C	Settling and Calming Section
D	Annular Passage Entrance
E	Annular Passage Test Section
F	Annular Passage Exit Section
G	Gate Valve
H	Hot-Wire Anemometer
I	Calming Screens
J	Honeycomb
K	Bell-mouth
L	Test Tube
M	Passage Entrance Section Inner
N	Iron Rod

Figure 2: Schematic Diagram of the Experimental Apparatus

Symbol	Definition
A	Nickel – Chrome heating
B	Test Tube
C	Magnesium Powder
D	Test Tuber surface
E	Thermocouples hot
F	Adhesive
G1 & G2	Conduction Heat loss
H1 & H2	Teflon pieces
I	Radiation heat loss
J	Velocity profile measuring
K	Exit temperature
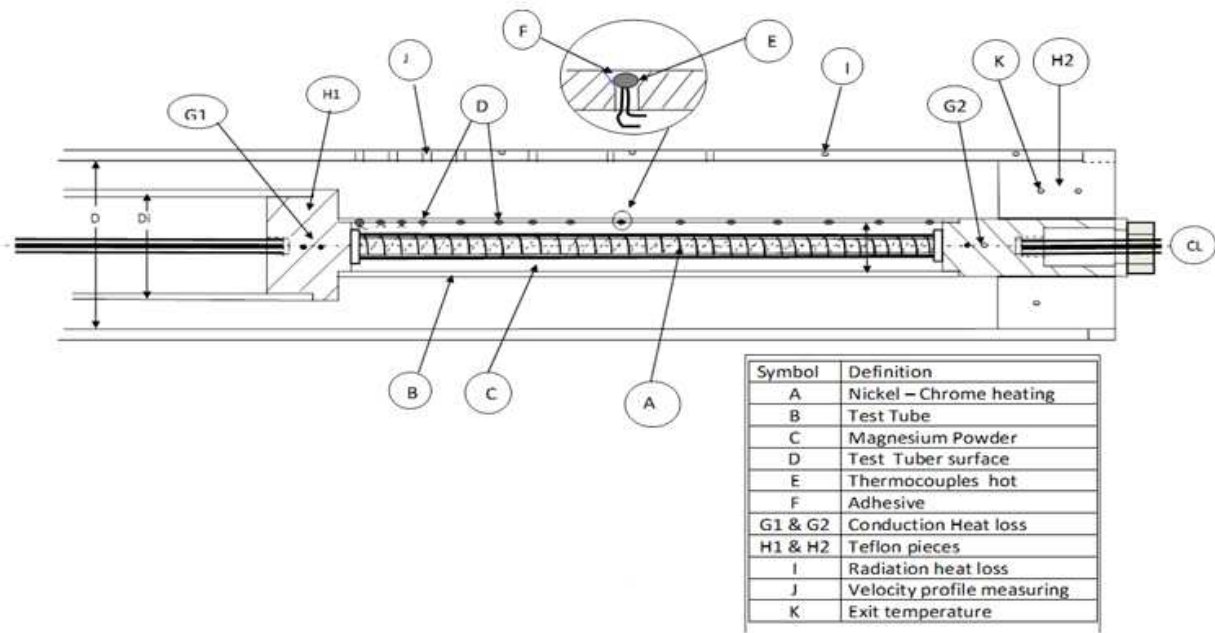
Figure 3: Test Section Heating and Measuring Systems Details
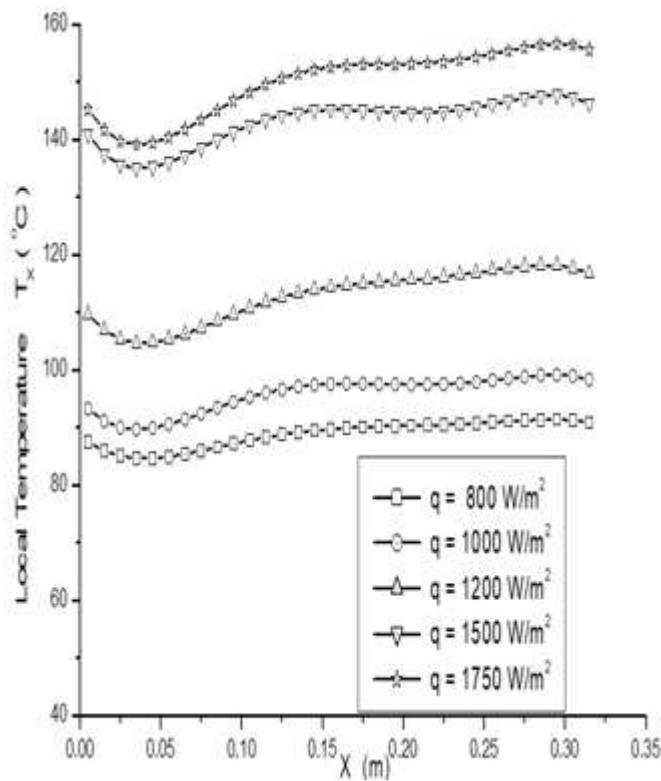
Figure 4: Variation of Local Temperature T_x along the Test Section Inner Tube.

(for Re = 3000 and D_i/d = 2.5)
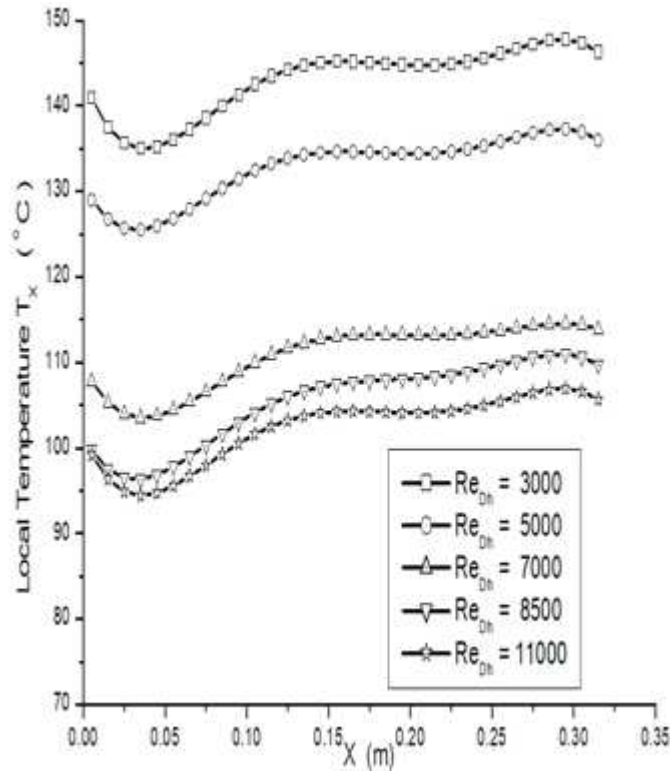
Figure 5: Variation of Local Temperature T$_x$ along the Test Section Inner Tube.

(for q = 1500 W/m^2 and D$_i$/d = 2.5)
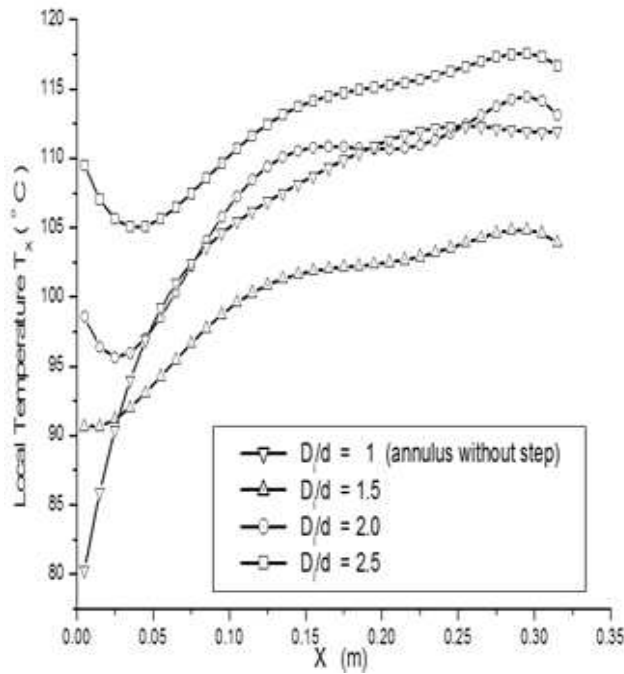
Figure 6: Variation of Local Temperature along the Test Section Inner Tube.

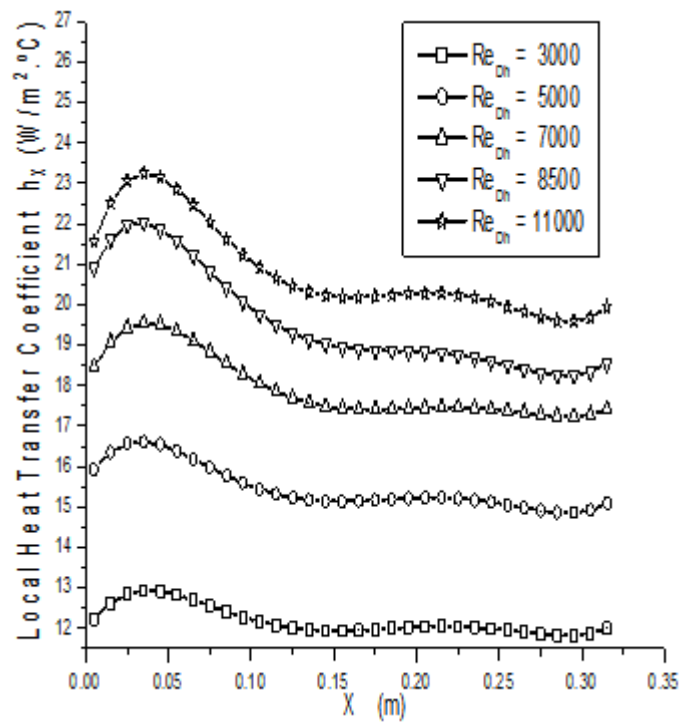**(for Re$_{Dh}$ = 11000 and q = 1750 W/m^2).**

Figure 7: Variation of Local Heat Transfer Coefficient along the Annulus Inner Tube
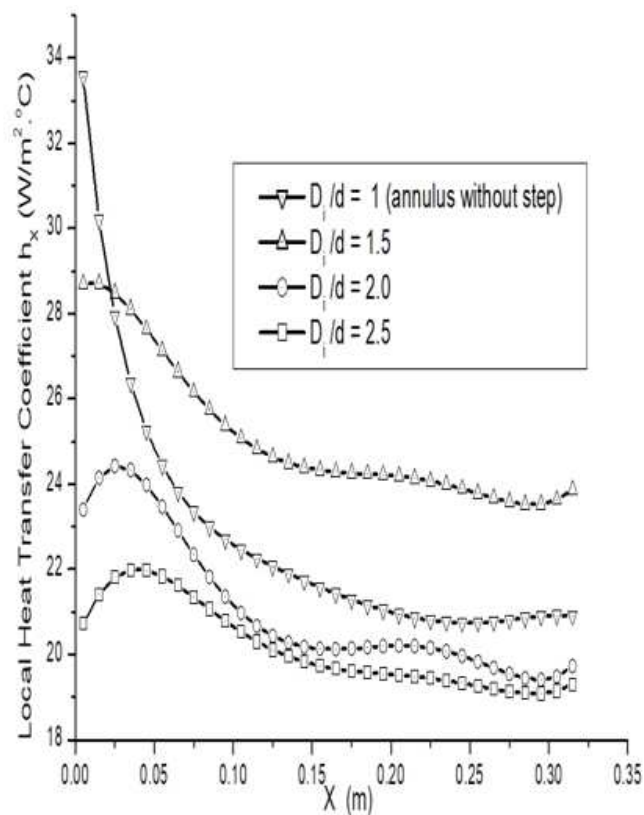
(for q = 1750 and D_i/d = 2.5)

Figure 8: Variation of Local Heat Transfer Coefficient h_x along the Annulus Inner Tube
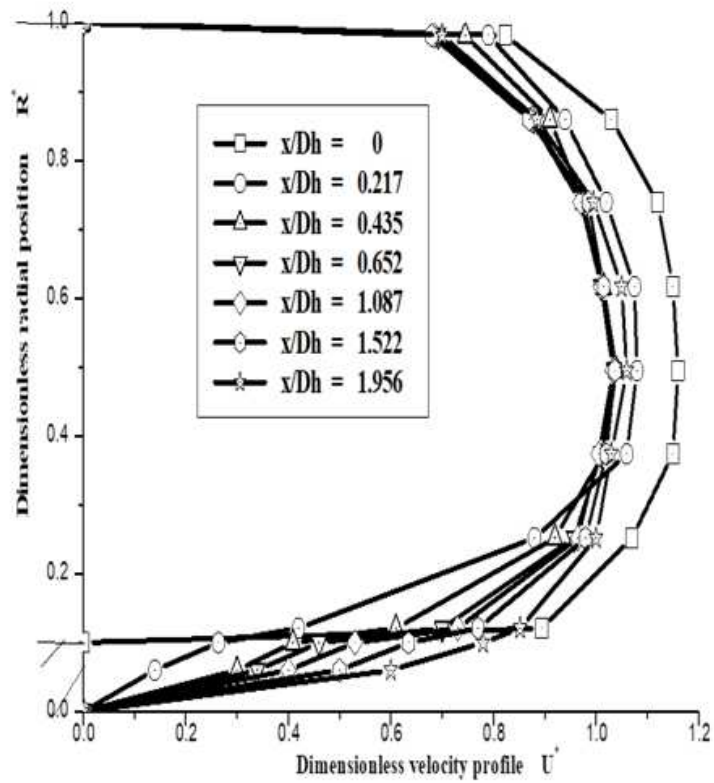
(for Re = 11000 and q = 1500 W/m^2).

Figure 9: Variation of Pitot Static Measurements of Axial Velocity Profiles along the Test Section Annular Passage
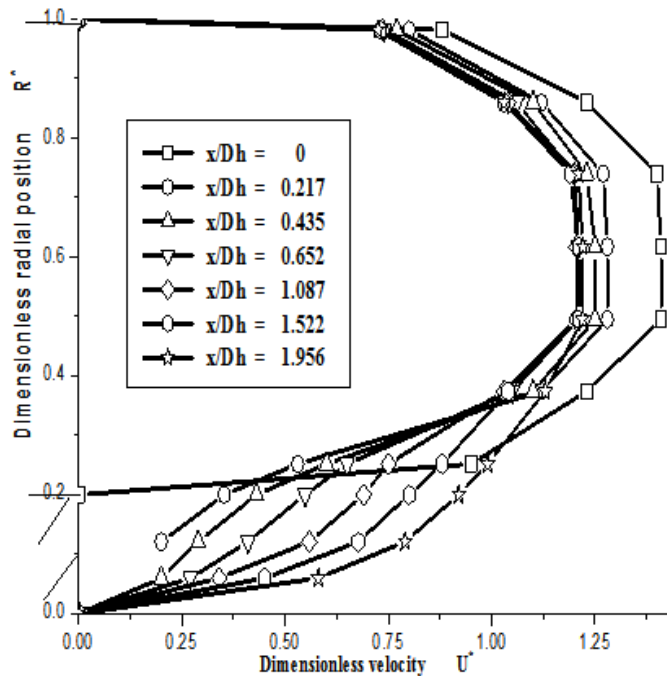
(for Re = 5000, q = 1750 W/m^2 and D$_i$/d = 1.5)

Figure 10: Variation of Pitot Static Measurements of Axial Velocity Profiles along the Test Section Annular Passage
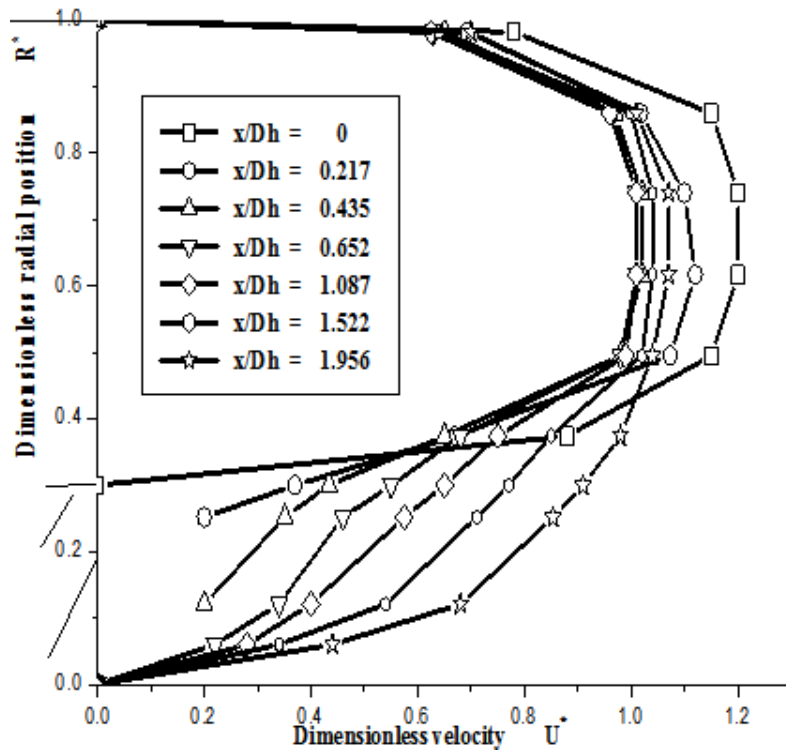
(for Re = 5000, q = 1750 W/m^2 and D$_i$/d = 2)

Figure 11: Variation of Pitot Static Measurements of Axial Velocity Profiles along the Test Section Annular Passage

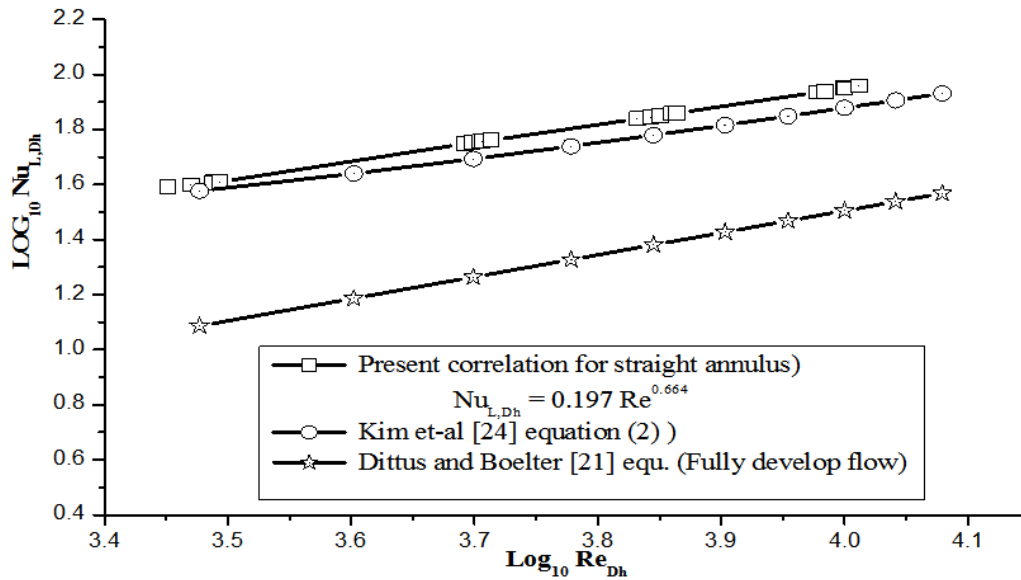**(for Re = 5000, q = 1750 W/m^2 and D_i/d = 2.5)**

Figure 12: Comparison of Present Straight Annular Correlating (without Step) with Ref [24] and Dittus and Boelter [21] for Fully Developed Flow Equation
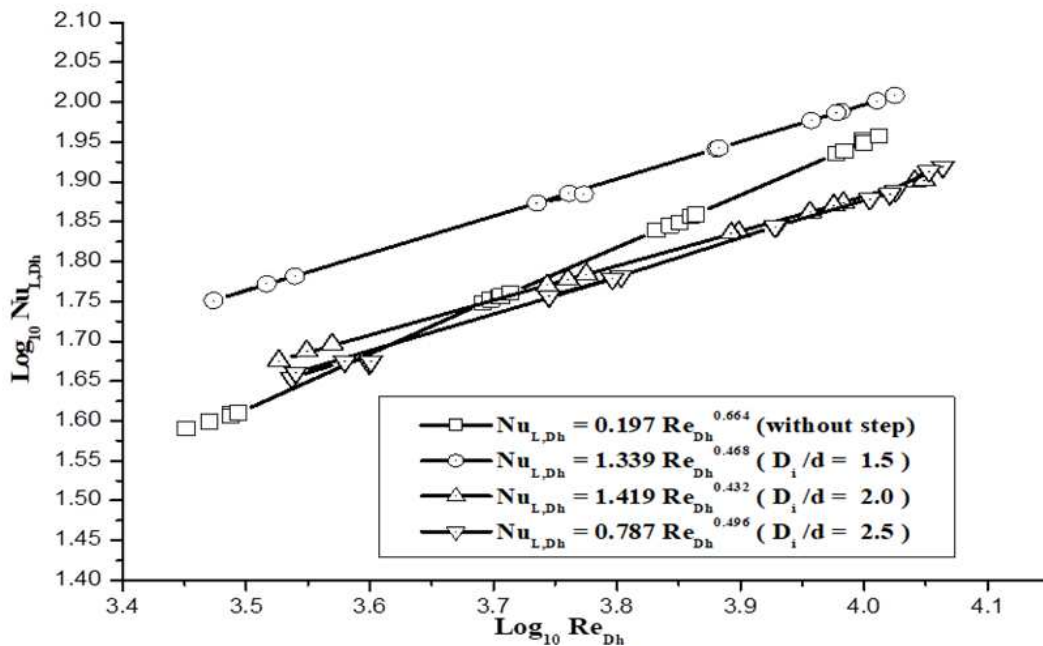
Figure 13: Comparison of Correlating between Average Nusselt Number with Reynolds Number for All Steps and the without Step Annular Passage

REFERENCES

1. *Wilcox, David C., (2007), 'Basic Fluid Mechanics". 3rd ed. Mill Valley: DCW Industries, Inc., 664-668.*

2. *Chang, P.K., (1970),' Separation of flow 'First edition, Headington Hill Hall.*

3. *Kiya, M., Mochizuk, O. Ishikawa, H. (1975). "Challenging Issues in separated and complex turbulent flows ". Hokkaido University, Sapporo, 060-8628; Japan.*

4. *Goldstein, R.J., Eriksen, V.L., Olsen, R.M., Eckert, E.R.G., (1970),'Laminar separation reattachment and transition of the flow over a downstream-facing step', Journal of Heat Transfer, ASME Transactions, Vol. 92, pp. 732–741.*

5. *Eaton,K., John,J.P. (1980) 'Turbulent flow reattachment: An experimental study of the flow and structure behind a backward-facing step.' Mech. Eng. Dep., Report No. MD - 39, Stanford University, Stanford, CA.*

6. *Popescu, F., Panait, T., (2007)'Numerical modelling and experimental validation of a turbulent separated reattached', International Journal of Mathematics and Computers in Simulation 1 (1) 7–11.*

7. *Adams,E.W., Eaton,J.K., (1988),'An LDA study of the backward-facing step flow, including the effects of the velocity bias', Journal of Fluids Engineering, Vol.110, pp. 275–282.*

8. *Jovic,S., (1996), 'An experimental study of a separated reattached flow behind a backward-facing step. Reh = 37000', NASA Technical Memorandum 110384,*

9. *Rouizi,Y., Favennec, Y., Ventura,J., PetitD., (2009)' Numerical model reduction of 2D steady incompressible laminar flows: application on the flow over a back ward facing step', Journal of Computational Physics, 228 (6), pp. 2239–2255.*

10. **Hall,E.J., Pletcher,R.H., (1985)** *'Application of a viscous–inviscid interaction procedure to predict separated flows with heat transfer', Journal of Heat Transfer, Vol. 107, pp. 557–563.*

11. **Habib,H.A.,McEligon,D.M.,(1980)**' *Turbulent heat transfer with swirl flow downstream of an abrupt pipe expansion.' Proc. of the 7-th Int. Heat Transfer Conf. 1982, Munich, V. 3, FC29.- PP. 159-166.*

12. **Vogel,J.C., Eaton,J. K.,(1985)**'* Combined heat transfer and fluid dynamic measurements down-stream of a backward-facing step.' Journal of Heat Transfer, ASME Transactions, Vol. 107, pp. 922–929.*

13. **Palm, R., Grundmann, S., Weismuller, M., Saric, S., Jakirlic, S., Tropea, C., (2006),**' *Experimental characterization and modelling of inflow, Vol. 27, pp. 924–936.*

14. **Kays, W.M., Leung,E.Y., (1963),** *'Heat transfer in annular passage – Hydro dynamically Developed Turbulent flow with arbitrarily prescribed Heat flux.' Journal of Heat and Mass Transfer, Vol. 6, pp.537–557.*

15. **Bsebsu,F.M. , Bede,G., (2002),**'*Theoretical study in single-phase forced-convection heat*

16. *transfer characteristics for narrow annuli fuel coolant channPolytechnica Series: Mechanical Engineering 46 , 15–27.*

17. **J.G. Barbosa Saldana, N.K. Anand, V. Sarin, (2005).** *'Forced convection over a three dimensional horizontal backward facing step', Int. Journal of Computational Engineering Science 6 225–234.*

18. **E.G. Filletti, W.M. Kays, (1967)."**Heat transfer in separated reattached and redevelopment regions behind a double step at entrance to a flat duct". Journal of Heat transfer, ASME 89, 163–168.*

19. **A. Davletshin, N.I. Mikheev, V.M. Molochnikov,(2008)."** Heat transfer in a turbulent separation region with superimposed stream pulsations"., J. of Thermo Physics and Aero mechanics 15 215–222.*

20. **E.M. Sparraw, J.P. Abraham, W.J. Minkowycz, (2009),**'*Flow separation in a diverging conical duct: effect of Reynolds number and divergence angle'. International Journal of Heat and Mass Transfer 52 (13–14) 3079– 3083.*

21. **Togun,H., Salman,Y.K., Aljibori,H. S. S., KaziS.N., (2011)**, *'An experimental study of heat transfer to turbulent separation fluid flow in an annular passage'International Journal of Heat and Mass Transfer 54 , 766 –773*

22. **Dittus, P. W., Boelter, S.N., (1985).**'*Heat Transfer in Automobile Radiators of the Tubular Type.' Univ. Calif. Pub. Eng., Vol. 2, No. 13, pp. 443-461 (1930), reprinted in Int. Comm. Heat Mass Transfer, Vol. 12, pp. 3-22.*

23. **Petukhov, B.S, Kurganov V.A., Gladuntsov A.I. (1970)** *'Heat transfer and friction in turbulent pipe flow with variable physical properties'. Adv. Heat Transfer 6, 503-565*

24. **Gnielinski, V., (1976)**, *Int. Chem. Engng , Vol. 16, pp. 359-368.*

25. **Kim W.S., Talbolt C. Chung B.J., Jackson J.D, (2002).**' *Variable property mixed convection heat transfer to air flowing through a vertical passage of annular cross section': Part 1, Trans.Int. Chem. Engng , Vol. 80, Part A pp.239-245.*

26. **Petukhov, B.S. and L.I. Roizen: (1964)**. *High Temperature 2, 65-68.*

NOMENCLATURE

Symbol	Description	Units
A_s	Test section inner tubeoutersurface area	[m^2]
C_p	Specific heat	[KJ/Kg.°K]
d	Test section inner tube outer diameter	[m]
Dh	Test sectionhydraulic diameter (Dh = (D-d))	[m]
Dh	Hydraulic diameter at entrance section (D_h=(D-D$_i$))	[m]
D	Whole annulus passage outer tube inner diameter	[m]
Di	Entrance section inner tube outer diameter (variable)	[m]
F	Annulus radiation shape factor	
h	Heat transfer coefficient	[W/m^2.°K]
I	Heater current	[Amp]
k	Thermal conductivity	[W/m.°K]
L	Test section whole length	[m]
Q	input power	[W]
q	Surface heat flux	[W/m^2]
r	Test section radial position measured from section center line	[m]
S	Step height	[m]
T	Temperature	[K]
U	Local air velocity	[m/s]
V	Heater voltage	[volt]
X	Axial distance after step	[m]

Dimensionless Group

Name	Description	
Nu$_{Dh}$	Local Nusselt number based on hydraulic diameter	(h_x.Dh/k)
Nu$_{max}$	Maximum Nusselt numberbased on hydraulic diameter	($h_{x,max}$.Dh/k)
Nu$_x$	Local Nusselt number based on axial distance	(h_x.X/k)
Nu$_{L,Dh}$	Average Nusselt numberbased on hydraulics diameter	(h_L.Dh/k)
Re$_{Dh}$	Reynolds number based on hydraulic diameter	(ρ.U.Dh/ μ)
Re$_x$	Local Reynolds number based on axial position	(ρ.U.X/ μ)
Re$_L$	Average Reynolds number	(ρ_L.U.Dh/ μ_L)
U*	Dimensionless axial velocity	(U/U$_i$)
R*	Dimensionless radial position	(2r-d)/Dh

Greek

Symbols	Description	Units
ρ	Air film density	(Kg/m^2)
μ	Air film dynamic viscosity	($Kg/m \cdot s$)
σ	Stephan-Boltzmann	($W/m^2 \cdot k^4$)
ε	Surface emissivity value	

Subscript

Subscript	Description
1,2	Outer surface of inner tube and inner surface of outer tube average
BX	Local air bulk
BL	Average air bulk
Cond.	Conductive
Conv.	Convection
FX	Local air film
FL	Average air film for l length
i	Annulus average inlet (upstream)
L	Average for whole length
max	Maximum local value
r	Radiation
SX	Local surface
SL	Average surface
X	local